NIH Public Access
Author Manuscript
Prostaglandins Other Lipid Mediat. Author manuscript; available in PMC 2014 June 11.

Published in final edited form as:
Prostaglandins Other Lipid Mediat. 2013 ; 0: 42–48. doi:10.1016/j.prostaglandins.2012.12.001.

Beneficial effects of inhibition of soluble epoxide hydrolase on glucose homeostasis and islet damage in a streptozotocin-induced diabetic mouse model

Lingdan Chen[a], **Cheng Fan**[a], **Yi Zhang**[a], **Mahinur Bakri**[b], **Hua Dong**[c], **Christophe Morisseau**[c], **Krishna Rao Maddipati**[d], **Pengcheng Luo**[e,f], **Cong-Yi Wang**[g], **Bruce D. Hammock**[c], and **Mong-Heng Wang**[a,*]

[a]Department of Physiology, Georgia Health Sciences University, Augusta, GA 30912, USA

[b]Xinjiang Key Laboratory of Plant Resources and National Products Chemistry, Xinjiang Technical Institution of Physics and Chemistry, Chinese Academy of Science, Urumqi 830011, PR China

[c]Department of Entomology and UCD Cancer Center, University of California, Davis, USA

[d]Department of Pathology, Wayne State University, Detroit, MI, USA

[e]Huangshi Central Hospital, Hubei Polytechnic University, Huangshi, Hubei Province 435000, PR China

[f]Huangshi Key Laboratory of Kidney and Metabolic Diseases, Huangshi, Hubei Province 435000, PR China

[g]Center for Biotechnology and Genomic Medicine, Georgia Health Sciences University, Augusta, GA 30912, USA

Abstract

Soluble epoxide hydrolase (sEH) is an enzyme involved in the metabolism of endogenous inflammatory and anti-apoptotic mediators. In the present study, we determined the effects of the inhibition of sEH on glucose homeostasis and islet damage in mice treated with streptozotocin (STZ), a model of chemical-induced diabetes. STZ increased daily water intake and decreased visceral (spleen and pancreas) weight in mice; sEH inhibition in STZ mice decreased water intake, but did not affect visceral weight. Hyperglycemia induced by STZ treatment in mice was attenuated by inhibiting sEH. The beneficial effects of sEH inhibition were accompanied, after 2 and 4 weeks of initial administration, by improving glucose tolerance. In contrast, sEH inhibition did not affect insulin tolerance. Using LC/MS analysis, neither STZ nor STZ plus sEH inhibition affected pancreatic and plasma ratios of epoxyeicosatrienoic acids (EETs) to dihydroxyeicosatrienoic acids (DHETs), an index of EETs levels. Western blot analysis showed that mouse cytochrome P450 (CYP) 2C enzymes are the major epoxygenases in islets. On day 5 after initial STZ treatment, STZ induced islet cell apoptosis, while sEH inhibition in STZ mice significantly reduced islet cell apoptosis. These studies provide pharmacological evidence that

© 2012 Elsevier Inc. All rights reserved.

*Corresponding author. Tel.: +1 706 721 3830; fax: +1 706 721 7299. mwang@georgiahealth.edu, (M.-H. Wang).

NIH-PA Author Manuscript
NIH-PA Author Manuscript
NIH-PA Author Manuscript

NIH-PA Author Manuscript

NIH-PA Author Manuscript

NIH-PA Author Manuscript

inhibiting sEH activity provides significant protection against islet β-cell damage and improves glucose homeostasis in STZ-induced diabetes.

Keywords

CYP-derived eicosanoids; Islets; Glucose homeostasis; Apoptosis

1. Introduction

The Centers for Disease Control estimates that the current annual cost of diabetes is $174 billion. Diabetes is characterized by hyperglycemia related to abnormalities in the function of pancreatic β cells, which is divided into type 1 (T1DM) and type 2 diabetes mellitus (T2DM). T1DM, which occurs in 5–10% of the diabetic patients, is characterized by autoimmune destruction of β-cells [1,2] and impairs quality of life because patients require daily insulin administration. T1DM also shortens life span as a consequence of cardiovascular disorders, including heart attack, hypertension, and stroke [3]. Obesity, which affects one in three Americans, is a serious health problem because it is often associated with T2DM [4,5], which occurs because of insulin resistance, a physiological condition in which peripheral tissues, including skeletal muscle and adipose tissue, are unable to respond efficiently to insulin [4,5]. Since both T1DM and T2DM are associated with cardiovascular and renal diseases, diabetes-associated complications result in major expense for families and impose a major societal economic burden.

Cytochrome P450 (CYP) enzymes constitute a major metabolic pathway for arachidonic acid (ArA). In the presence of NADPH and oxygen, ArA is oxidized by CYP 2C and 2J epoxygenases into four epoxyeicosatrienoic acids, 5,6-EET, 8,9-EET, 11,12-EET, and 14,15-EET [3]. During the past two decades, it has been recognized that EETs have important biological effects in the kidneys, including inhibition of sodium transport in the nephron and vasodilation of renal arterioles [6]. In the renal vasculature, EETs cause vasodilation of renal arterioles and function as endothelial-derived hyperpolarizing factors [7,8]. However, EETs can be hydrolyzed by soluble epoxide hydrolase (sEH) to the corresponding dihydroxyeicosatrienoic acids (DHETs). It has been shown that DHETs have much less biological activity than do EETs, and are rapidly conjugated and excreted [8–10]. Therefore, inhibition of sEH activity has been used as a means of studying the biological functions of EETs [8,11].

Recently, it has been shown that sEH has functional implication in both STZ-induced diabetes [12] and a high-fat diet model [13]. For example, using a hyperglycemic clamp approach, Luo et al. [12] have shown that sEH knockout promotes insulin secretion in vivo, thus preventing hyperglycemia in STZ-induced diabetes. Moreover, using pharmacological inhibitor and knockout of sEH, Luria et al. [13] have demonstrated that inhibition and deletion of sEH in mice attenuate high-fat diet-induced insulin resistance and improve glucose tolerance by enhancing tyrosyl phosphorylation of the insulin receptor, insulin receptor substrate, and their downstream cascade.

NIH-PA Author Manuscript

NIH-PA Author Manuscript

NIH-PA Author Manuscript

Although it is well established that sEH inhibition has beneficial effects in cardiovascular, renal, and inflammatory diseases, its contribution to glucose homeostasis and islet function in diabetes is still not clear. Therefore, our objective in the present study was to further characterize the effects of *trans*-4-[4–(3-adamantan-1-ylureido)-cyclohexyloxy]-benzoic acid (*t*-AUCB), a potent sEH inhibitor, in an STZ-induced diabetic mouse model, in an effort to define the protective effects of sEH inhibition in glucose homeostasis and islet damage during diabetes.

2. Materials and methods

2.1. Animals

Male 8-week-old C57BL/6J mice (Jackson Laboratory, Bar Harbor, ME) were divided into 3 groups. The control group consisted of mice given vehicle; the multiple low-dose STZ (MLD-STZ) group consisted of mice given 5 intraperitoneal doses of 40 mg/kg of STZ in citrate buffer (pH 4.5) plus daily injection of vehicle; the STZ + *t*-AUCB group consisted of mice given MLD-STZ for 5 days and *t*-AUCB (5 mg/kg/day, ip) for 4 weeks. Daily water and food intake were recorded after STZ treatment. To determine weekly blood glucose concentration, mice were fasted for 3 h, from 8:00 am to 11:00 am. We then measured their glucose levels with a glucometer (Accu-Check blood glucose monitor system, Roche Diagnostics, Indianapolis, IN) after their different treatments. To determine 24-h urine volume, mice given different treatments for 4 weeks were placed in individual metabolic cages for urine collection, and urine glucose levels were determined by Diastrix strips (Bayer Health Care, Mishawaka, IN). Mice to be euthanized after 4 weeks of different treatments were deeply anesthetized with triple anesthetic combination (1.9 mg/ml xylazine, 0.37 mg/ml acepromazine, and 37.5 mg/ml ketamine), then underwent thoracotomy. Mouse spleens and pancreases were collected and weighed. Through studies, all mice were maintained on a 12:12-h light–dark cycle and were housed 5 mice to a cage. All animal protocols were approved by the Institutional Animal Care and Use Committee and were in accord with the requirements of the National Institute of Health Guide for the Care and Use of Laboratory Animals.

2.2. Intraperitoneal glucose tolerance test and insulin tolerance test

After 2 or 4 weeks of the different treatments, mice were given an intraperitoneal glucose tolerance tests (IGTT). After mice had fasted for 6 h, blood glucose concentrations were measured first from the tail vein. Four more blood glucose concentrations per mouse were determined at 15-, 30-, 60-, and 120-min intervals after the injection of glucose (1 g/kg, ip). An insulin tolerance test was done similarly, by injecting human insulin (1 U/kg, ip). Four blood glucose concentrations were determined before or at 10-, 30-, and 60-min intervals after insulin administration. The values of area under the curve for blood glucose ($AUC_{glucose}$) in IGTT and insulin tolerance test were determined by GraphPad Software (San Diego, CA). The protocols for IGTTs and insulin tolerance tests have been described previously [12].

NIH-PA Author Manuscript

NIH-PA Author Manuscript

NIH-PA Author Manuscript

2.3. Pancreatic and plasma ratios of EETs to DHETs, determined by liquid chromatography–mass spectrometry (LC–MS) analysis

Since our preliminary data indicated that we cannot detect EETs and DHETs levels from islets isolated from mice (data not shown), we decided to determine pancreatic rather than islet EETs and DHETs levels. Using HEPEs buffer, we homogenized pancreatic samples isolated from the experimental groups. We then incubated pancreatic samples with 5 μM ArA for 1 h at 37 °C. We added ArA to pancreatic samples to enhance EETs production; this protocol is to determine epoxygenase activity rather than endogenous EETs levels. After brief centrifuging, the supernatants of samples were kept at −80 °C. Samples were spiked with 10 ng of 15(S)-HETE-d_8, applied to preconditioned SEP-Pak C18 cartridges (100 mg adsorbent, Waters), then washed with water followed by hexane. Eicosanoids were eluted with 500 μl of ethyl acetate–hexane (3:1). The eluate was dried under nitrogen and reconstituted in methanol: 25 mM aqueous ammonium acetate (7:3). The extracted and reconstituted sample was subjected to HPLC (Shimadzu Prominence XR system) on a Max-RP C18 column (2 × 150 mm, 3 μ, Phenomenex) eluted isocratically with methanol: 13 mM aqueous ammonium acetate (8:2) at a flow rate of 0.4 ml/min. The eluent was monitored for EETs and DHETs by mass spectrometer (QTRAP5500, ABSCIEX) in the negative ion mode using Multiple Reaction Monitoring under optimized conditions for the transitions of *m/z* 155 for 8,9-EET, *m/z* 167 for 11,12-EET, and *m/z* 219 for 14, 15-EET, as well as the transitions of *m/z* 337 to *m/z* 145 for 5,6-DHET, *m/z* 167 for 11,12-DHET, *m/z* 185 for 8,9-DHET, and *m/z* 207 for 14,15-DHET (ionization potential: −1500, source temperature: 600 °C, curtain gas and GS1: 35 psi, GS2: 65 psi, declustering potential: −60 V, entrance potential: −7 V, collision energies: 17–22 eV, and collision cell exit potentials: 7.6–11 eV). 15(S)-HETE-d_8 (MRM transition of *m/z* 327–226 under identical conditions) was used as the internal standard for recovery and quantitation. Under these conditions, retention times were: 15-HETE (and 15(S)-HETE-d_8): 2.57 min; 14,15-EET: 3.08 min; 11,12-EET: 3.38 min; 8,9-EET: 3.56 min; 14,15-DHET: 1.92 min; 11,12-DHET: 2.08 min; 8,9-DHET: 2.36 min; and 5,6-DHET: 2.77 min. Under these conditions, the minimum detection limit was 50 pg for each compound on the column. The concentrations of EETs and DHETs in pancreatic samples were normalized with protein concentration as described previously [14]. The concentrations of *t*-AUCB in the pancreatic samples, as well as plasma EETs and DHETs levels, were determined by LC–MS as described previously [15].

2.4. Pancreatic islet isolation

Pancreatic islets were isolated by a modified collagenase digestion method as previously described [16,17]. Anesthetized 8-week-old male mice were sacrificed by cervical dislocation. The common duct was clamped at its entrance to the duodenum and cannulated under a dissecting microscope. Pancreatic inflation was accomplished via the bile duct with 2.0–2.5 ml of 0.5 mg/ml collagenase XI (Roche, Indianapolis, IN) dissolved in Hank's buffer supplemented with 1 mM $MgCl_2$ and 10 mM HEPEs. The distended pancreases were removed and incubated with type XI collagenase (Roche, Indianapolis, IN) in glass vials for about 17 min at 37 °C. During the incubation, we manually agitated the glass vials to achieve tissue disintegration. We isolated islets under a dissecting microscope, and

NIH-PA Author Manuscript

NIH-PA Author Manuscript

NIH-PA Author Manuscript

estimated that we had obtained about 80–100 islets per mouse. The protocol of pancreatic islet isolation has been described previously [12].

2.5. Western blot analysis

Expression of CYP2C11, CYP2J, sEH, and β-actin was analyzed in homogenized samples isolated from 8-week-old mice. Renal and islet samples were separated by NuPAGE 4–12% Bis–Tris gel (Invitrogen, Carlsbad, CA) at 125 V for 3 h. We have previously described the detailed procedures for transfer, blocking, and washing the samples [18]. The membranes were incubated with antibody against CYP2C11 (1:1000; Fitzgerald Industries International, Concord, MA), CYP2J (1:200; Santa Cruz Biotechnology, Santa Cruz, CA), human sEH (1:1000), or β-actin (1:5000; Sigma, St. Louis, MO). The membranes were incubated with secondary antibody for CYP2C11, CYP2J, sEH, or β-actin. We developed the immunoblots using an ECL detection kit (GE Healthcare, Little Chalfont, Buckinghamshire, UK).

2.6. Terminal deoxynucleotidyl transferase-mediated deoxyuridine triphosphate nick-end labeling (TUNEL) staining

Eight-week-old male mice were treated with vehicle, STZ (40 mg/kg/day for 5 days, ip), or STZ plus *t*-AUCB (5 mg/kg/day for 5 days, ip). Mice given these treatments were sacrificed on day 5 (day 1 corresponding to the day of first STZ injection). Mouse pancreases were isolated, fixed, sectioned, and TUNEL stained. The TUNEL assay was done using the ApopTag Plus Peroxidase In Situ Apoptosis Detection Kit (Millipore, Temecula, CA) according to the manufacturer's instructions. The slides with TUNEL staining were viewed in a blinded manner. The number of TUNEL-positive cells was determined from mouse pancreas in all experimental groups. Apoptosis was scored as the average number of TUNEL-positive cells per islet size (1000 μm^2). Islet size was determined using the National Institutes of Health Image J software (http://rsb.info.nih.gov/ij/).

2.7. Statistical analysis

All values are expressed as means ± SE. All data were analyzed by GraphPad Instat Software (LaJolla, CA). We used one-way ANOVA and Tukey–Kramer tests for multiple comparisons or independent Student's *t* test for unpaired groups. Statistical significance was set at $P < 0.05$, 0.01, or 0.001.

3. Results

Effects of sEH inhibition on daily water intake, daily food intake, visceral weight, urine volume, and urine glucose in STZ-diabetic mice

To evaluate whether treatment with *t*-AUCB, a potent sEH inhibitor, affects 24-h urine volume, food intake, or visceral weight (spleen and pancreas) in diabetes, we induced diabetes in male C57BL/6J mice by injecting them with MLD-STZ (40 mg/kg/day of STZ for 5 days, ip). Treatment with neither STZ (21.3 ± 0.5 vs. 21 ± 0.5 g, $n = 6$) nor STZ + *t*-AUCB (20.8 ± 0.7 vs. 21 ± 0.5 g, $n = 6$) affected body weight. As shown in Fig. 1, as compared to the control group, mice treated with STZ had significantly increased the average of their daily water intake in the entire treatment time (Fig. 1A); STZ treatment also

NIH-PA Author Manuscript

NIH-PA Author Manuscript

NIH-PA Author Manuscript

decreased visceral weight (Fig. 1C; $P \leq 0.05$). When STZ mice were co-treated with *t*-AUCB (5 mg/kg/day, ip) for 4 weeks, it normalized their daily water intake (Fig. 1A; $P \leq 0.001$), but did not affect visceral weight in STZ mice (Fig. 1C). Neither STZ nor STZ plus *t*-AUCB treatment affected food intake (Fig. 1B).

In a complementary experiment, STZ-treated mice had significant higher 24-h urine volume (8.3 ± 2.6 vs. 1.1 ± 0.3 ml/day, $n = 5$, $P < 0.01$) and urine glucose (300 ± 112 vs. 0 mg/dl, $n = 5$) than the corresponding values in control mice, when co-treatment with *t*-AUCB in STZ mice, it significantly reduced 24-h urine volume (2.9 ± 0.7 vs. 8.3 ± 2.6 ml/day, $n = 5$, $P < 0.01$) and urinary glucose levels (110 ± 89 vs. 300 ± 112 mg/dl, $n = 5$, $P < 0.05$).

3.1. Effects of sEH inhibition on glucose tolerance and insulin tolerance in STZ-diabetic mice

Since STZ acts very quickly on β-cell loss [19], we investigated if sEH inhibition prevents the early stage of β-cell damage and affects glucose homeostasis by STZ treatment. Thus, we concurrently treated mice with both STZ and *t*-AUCB. Weekly blood glucose levels were measured in separate cohorts of mice. After administration of STZ, mice showed significant hyperglycemia during week 1 ($P < 0.05$), week 2 ($P < 0.001$), week 3 ($P < 0.01$), and week 4 ($P < 0.001$) (Fig. 2). Concurrent treatment with STZ and *t*-AUCB (5 mg/kg/day) significantly decreased hyperglycemia during week 1 ($P < 0.01$), week 2 ($P < 0.01$), week 3 ($P < 0.05$), and week 4 ($P < 0.01$) (Fig. 2).

To elucidate the contribution of sEH inhibition on glucose and insulin homeostasis in STZ-induced diabetes, we investigated the effects of *t*-AUCB treatment on IGTT and insulin tolerance tests at weeks 2 and 4 after initial STZ treatment in separate cohorts of mice. At week 2 after STZ treatment, $AUC_{glucose}$ of IGTT in STZ-treated mice was significantly higher than that in control mice ($P < 0.001$) (Fig. 3B), while $AUC_{glucose}$ of IGGT in the STZ plus *t*-AUCB group was significantly lower than that in the STZ group ($P < 0.001$) (Fig. 3B). Similar effects by STZ ($P < 0.01$) and STZ plus *t*-AUCB ($P < 0.01$) treatments in $AUC_{glucose}$ of IGTT were observed at week 4 after STZ treatment (Fig. 4B). In contrast, after initial STZ treatment, co-treatment with *t*-AUCB did not affect insulin tolerance in STZ-diabetic mice at week 2 or week 4 (Figs. 3C and 4C).

3.2. Effects of sEH inhibition on pancreatic and plasma ratios of EETs to DHETs and expression of CYP epoxygenases and sEH in mouse islets

To evaluate whether sEH inhibition affects EETs levels in the pancreas, we determined pancreatic ratios of EETs to DHETs, a parameter that indicates in vivo sEH inhibition and is commonly used for targeting epoxygenases, by LC–MS analysis. Neither STZ nor STZ plus *t*-AUCB treatment affected pancreatic ratios of EETs to DHETs (Fig. 5A). To evaluate whether *t*-AUCB present in the pancreas after chronic treatment with *t*-AUCB, we determined the concentrations of *t*-AUCB by LC–MS in the pancreatic samples isolated from STZ and STZ plus *t*-AUCB groups. We did not find any *t*-AUCB in STZ group, but the levels of *t*-AUCB in STZ plus *t*-AUCB group were 99 ± 22 ng/g of tissue weight ($n = 4$). To evaluate whether *t*-AUCB treatment affect circulating EETs levels, we determined

NIH-PA Author Manuscript

NIH-PA Author Manuscript

NIH-PA Author Manuscript

plasma ratios of EETs to DHETs in control, STZ, and STZ plus *t*-AUCB group. Neither STZ nor STZ plus *t*-AUCB treatment affected plasma ratios of EETs to DHETs (Fig. 5B).

Since significant amounts of EETs and DHETs are produced in the pancreas (Fig. 5A), we determined what major CYP enzymes are responsible for EETs synthesis in islets. We isolated mouse islets using a modified collagenase digestion method, images of representative isolated islets are shown in Fig. 5C. We then determined the expression levels of CYP2C11, CYP2J, and sEH in the kidneys and islets by loading the same amount of protein in Western blot analyses. As shown in Fig. 5D, greater expression of CYP2J and sEH expression was found in kidneys than in islets, whereas greater expression of CYP2C11 was found in islets than in kidneys.

3.3. Effects of sEH inhibition on islet apoptosis in STZ-diabetic mice

It is well established that loss of β-cells through apoptosis is an important factor in causing hyperglycemia in the MLD-STZ model; early induction of apoptosis occurs on day 5 after initial STZ administration [19,20]. Thus, we decided to determine whether sEH inhibition protects β-cells from the early stage of damage. To examine islet apoptosis, we did terminal deoxynucleotidyl transferase-mediated deoxyuridine triphosphate nick-end labeling (TUNEL) staining on day 5 after the initial STZ injection in separate cohorts of mice. As shown in Fig. 6A, we did not observe any apoptosis in pancreatic sections from control mice. MLD-STZ treatment significantly induced islet cell apoptosis, but treatment with *t*-AUCB in STZ mice significantly reduced islet cell apoptosis ($P < 0.05$) (Fig. 6B).

4. Discussion

Diabetes is characterized by hyperglycemia, which is related to abnormalities in the function of pancreatic β cells. Because pancreatic dysfunction and β-cell death are important factors in the pathogenesis of diabetes, diminishing β-cell dysfunction and preventing β-cell death are important strategies to enhance glucose homeostasis in diabetes [21]. In this study, we used MLD-STZ to induce diabetes [19]. Since sEH is an enzyme involved in the metabolism of endogenous inflammatory and anti-apoptotic mediators [3], we hypothesized that sEH inhibition might prevent hyperglycemia and protect against islet damage in STZ mice. We found that MLD-STZ caused hyperglycemia, which was associated with increased 24-h urine volume and urine glucose, impaired glucose tolerance, and increased islet apoptosis. Concurrent treatment of STZ mice with *t*-AUCB reduced hyperglycemia, 24-h urine volume, urine glucose, and islet apoptosis as well as improving glucose tolerance. Thus, sEH inhibition prevents STZ-induced hyperglycemia by improving glucose homeostasis and reducing β-cell death.

In this study, we showed that *t*-AUCB treatment improved glucose tolerance, but did not affect insulin tolerance (Figs. 3 and 4). These results support the notion that the anti-hyperglycemic effects of *t*-AUCB are largely attributable to the improvement of glucose tolerance, which occurs as a result of improved ability of islets to release insulin following intraperitoneal glucose administration. Mechanistically, one of our previous studies suggested that sEH knockout promotes insulin secretion by an amplifying pathway [12].

NIH-PA Author Manuscript

NIH-PA Author Manuscript

NIH-PA Author Manuscript

Thus, it is possible that sEH inhibition by *t*-AUCB also promotes insulin secretion through a similar mechanism.

In the present study, we found that the administration of *t*-AUCB did not affect pancreatic ratios of EETs to DHETs (Fig. 5A), an index of in vivo sEH inhibition in the pancreas. Several studies have suggested that sEH inhibition increases EETs levels by decreasing the degradation of EETs [22,23]. In accordance with this view, Liu et al. [15] have shown that *t*-AUCB treatment reduces the production of DHETs and increases the ratios of EETs to DHETs in the plasma of lipopolysaccharide (LPS)-treated mice. However, *t*-AUCB treatment did not affect plasma ratios of EETs to DHETs in STZ mice (Fig. 5B). The reason for the inconsistency between previous results [15] and our results (Fig. 5B) with respect to plasma EETs/DHETs ratios after *t*-AUCB treatment is not known, but could be a consequence of either procedural differences such as different doses and different duration of treatment or different animal models (LPS versus STZ).

t-AUCB treatment did not affect both pancreatic (Fig. 5A) and plasma ratios (Fig. 5B) of EETs to DHETs, suggesting that the protective effects of sEH inhibition on pancreatic dysfunction are not due to the elevation of EETs levels. Therefore, the exact mechanisms whereby sEH inhibition prevents hyperglycemia and β-cell death are still unknown. However, this prevention could occur as a consequence of the function of sEH on other lipid mediators. It is well established that, besides arachidonic acid, CYP epoxygenases catalyze the formation of epoxygenated fatty acids (EFAs) from fatty acids, which include linoleic, linolenic, docosahexaenoic, and eicosapentaenoic acid [24,25]. EFAs are further metabolized by sEH into their corresponding diol products. It is well known that EFAs have strong anti-inflammatory effects [24,25]. Thus, inhibition of sEH by *t*-AUCB could stabilize levels of free EFAs in plasma and tissue levels, which may prevent hyperglycemia and improve pancreatic function of STZ mice through anti-inflammatory mechanism.

Although the promotion of insulin secretion by sEH inhibition is an important component in the reduction of hyperglycemia in STZ mice, other biological activities generated as a result of sEH inhibition can contribute to this beneficial effect. It is well established that the MLD-STZ model causes β-cell loss through apoptosis, which leads to hyperglycemia [19,20]. Since sEH inhibitor reduces the expression of proapoptotic genes in neural tissue [26], we hypothesize that the prevention of hyperglycemia by *t*-AUCB is the result of its anti-apoptotic properties. To test this hypothesis, we set out to determine whether sEH inhibition affects islet cell apoptosis in the MLD-STZ model, finding that the *t*-AUCB + STZ group had less islet cell apoptosis than did the STZ group (Fig. 6). These findings are consistent with our earlier study [12], in which sEH knockout also reduced islet cell apoptosis in STZ-induced diabetes. Taken together, these results demonstrate that the anti-apoptotic property of sEH inhibitor is an important mechanism in preventing hyperglycemia in the MLD-STZ model. Although sEH inhibition significantly reduced islet cell apoptosis (Fig. 6), the mechanism whereby the treatment of *t*-AUCB reduces islet apoptosis in STZ mice is still not known. Since sEH is involved in the degradation of EFAs, treatment of *t*-AUCB could increase the circulating levels of these lipid mediators. Thus, it is possible that these upstream EFAs may act as anti-apoptotic factors to protect islets from STZ-induced damage.

NIH-PA Author Manuscript

NIH-PA Author Manuscript

NIH-PA Author Manuscript

Although there is significant EETs production in the pancreas (Fig. 5A), the major enzymes responsible for EETs production in the islets are still not clear. It is known that EETs biosynthesis can be carried out by several isoforms, including the CYP1A, CYP2B, CYP2C, and CYP2J families [27]. Although many CYP enzymes can epoxidize ArA, it is widely accepted that CYP2C and CYP2J are the primary enzymes responsible for EET synthesis [28]. Mouse CYP2C and CYP2J isoforms are highly expressed in different tissues, including liver, kidneys, and brain [27]. However, the expression pattern of these CYP2C and CYP2J isoforms in islets is unknown. In this study, we used CYP2C11 and CYP2J antibodies to determine the expression levels of these enzymes in kidneys and islets. We found that CYP2J isoforms are more highly expressed in kidneys than in islets (Fig. 5), whereas CYP2C11-like isoforms are more highly expressed in islets than in kidneys (Fig. 5). Since mouse CYP2C isoforms are highly active epoxygenases [27], these results suggest that mouse CYP2C enzymes, rather than CYP2J enzymes, are responsible for EET synthesis in islets. However, future investigation with real-time PCR is needed to establish which CYP2C isoform is the major epoxygenase in islets.

Our finding that *t*-AUCB reduces hyperglycemia and islet damage in STZ-induced diabetes may have significant clinical implications because polymorphism of sEH is associated with clinical parameters in diabetic patients. For example, Ohtoshi et al. [29], by determining the genotype distribution and allele frequency of sEH gene G860A (Arg287Gln) polymorphism in Japanese subjects, have shown that this polymorphism is closely associated with insulin resistance in T2DM patients. To facilitate the development of sEH inhibitors for clinical studies, Chen et al. [30] evaluated the safety, pharmacokinetics, and pharmacodynamics of AR9281, a potent sEH inhibitor, in healthy subjects. They found that AR9281 inhibits sEH activity by 90% in these subjects without having significant adverse events. In addition, sorafenib, a drug used to treat renal cell carcinoma, effectively inhibits sEH activity in vivo [31]. Thus, it will be important to see if randomized, double-blinded, placebo-controlled clinical studies using sEH inhibitors such as *t*-AUCB, AR9281, or sorafenib will prevent hyperglycemia and improve glucose tolerance in T1DM and T2DM patients.

5. Conclusions

Our results demonstrate that inhibition of sEH activity by *t*-AUCB decreases hyperglycemia, 24-h urine volume, and urine glucose in STZ-induced diabetes. Our glucose tolerance and insulin tolerance results support the notion that reduction of hyperglycemia by *t*-AUCB treatment is mediated by improving glucose tolerance. Because *t*-AUCB treatment did not affect the pancreatic and plasma ratios of EETs to DHETs, our results did not support the notion that increasing EETs levels are responsible for the beneficial effects of sEH inhibitor in STZ-induced diabetes. The mechanism for the protective effects of *t*-AUCB treatment on the pancreas is still not clear and requires further investigation. Our biochemical analysis demonstrated that CYP2C isoforms are the major epoxygenases in islets. Since *t*-AUCB treatment significantly decreased STZ-induced islet apoptosis, it is also possible that the reduction of hyperglycemia by sEH inhibition is mediated through the reduction of β-cell loss. Therefore, blockade of sEH activity by pharmacological inhibitors could be an effective approach to the successful control of hyperglycemia in diabetes.

NIH-PA Author Manuscript

NIH-PA Author Manuscript

NIH-PA Author Manuscript

Acknowledgments

The authors thank Jeanne D. Cole for editorial assistance. *Grant*: This study was supported by AHA Grant-in-Aid grant (AHASE0054) and GHSU intramural grant (DODI Synergy Award) to M.H. Wang. Partial support was provided by National Institutes of Health grant (ES-002710) to B.D. Hammock, and National Natural Science Foundation of China (NSFCN81000341) to P. Luo.

References

1. Yoon JW, Jun HS. Autoimmune destruction of pancreatic beta cells. Am J Ther. 2005; 12:580–591. [PubMed: 16280652]
2. Cnop M, Welsh N, Jonas JC, Jörns A, Lenzen S, Eizirik DL. Mechanisms of pancreatic beta-cell death in type 1 and type 2 diabetes: many differences, few similarities. Diabetes. 2005; 54:S97–S107. [PubMed: 16306347]
3. Luo P, Wang MH. Eicosanoids, beta-cell function, and diabetes. Prostaglandins Other Lipid Mediat. 2011; 95:1–10. [PubMed: 21757024]
4. Boden G. Obesity, insulin resistance and free fatty acids. Curr Opin Endocrinol Diabetes Obes. 2011; 18:129–143. [PubMed: 21297468]
5. Eckardt K, Taube A, Eckel J. Obesity-associated insulin resistance in skeletal muscle: role of lipid accumulation and physical inactivity. Rev Endocr Metab Disord. 2011; 12:163–172. [PubMed: 21336841]
6. Zhao X, Imig JD. Kidney CYP450 enzymes: biological actions beyond drug metabolism. Curr Drug Metab. 2003; 4:73–84. [PubMed: 12570747]
7. Imig JD. Eicosanoids and renal vascular function in diseases. Clin Sci. 2006; 111:21–34. [PubMed: 16764555]
8. Imig JD. Epoxide hydrolase and epoxygenase metabolites as therapeutic targets for renal diseases. Am J Physiol. 2005; 289:F496–F503.
9. Deng Y, Theken KN, Lee CR. Cytochrome P450 epoxygenases, soluble epoxide hydrolase, and the regulation of cardiovascular inflammation. J Mol Cell Cardiol. 2010; 48:331–341. [PubMed: 19891972]
10. Imig JD, Hammock BD. Soluble epoxide hydrolase as a therapeutic target for cardiovascular diseases. Nat Rev Drug Discov. 2009; 8:794–805. [PubMed: 19794443]
11. Imig JD. Cardiovascular therapeutic aspects of soluble epoxide hydrolase inhibitors. Cardiovasc Drug Rev. 2006; 24:169–188. [PubMed: 16961727]
12. Luo P, Chang HH, Zhou Y, Zhang S, Hwang SH, Morisseau C, et al. Inhibition or deletion of soluble epoxide hydrolase prevents hyperglycemia, promotes insulin secretion, and reduces islet apoptosis. J Pharmacol Exp Ther. 2010; 334:430–438. [PubMed: 20439437]
13. Luria A, Bettaieb A, Xi Y, Shieh GJ, Liu HC, Inoue H, et al. Soluble epoxide hydrolase deficiency alters pancreatic islet size and improves glucose homeostasis in a model of insulin resistance. Proc Natl Acad Sci USA. 2011; 108:9038–9043. [PubMed: 21571638]
14. Maddipati KR, Zhou SL. Stability and analysis of eicosanoids and docosanoids in tissue culture media. Prostaglandins Other Lipid Mediat. 2011; 94:59–72. [PubMed: 21236355]
15. Liu JY, Tsai HJ, Hwang SH, Jones PD, Morisseau C, Hammock BD. Pharmacokinetic optimization of four soluble epoxide hydrolase inhibitors for use in a murine model of inflammation. Br J Pharmacol. 2009; 156:284–296. [PubMed: 19154430]
16. Oshima H, Taketo MM, Oshima M. Destruction of pancreatic beta-cells by transgenic induction of prostaglandin E2 in the islets. J Biol Chem. 2006; 281:29330–29336. [PubMed: 16873378]
17. Zhang CY, Baffy G, Perret P, Krauss S, Peroni O, Grujic D, et al. Uncoupling protein-2 negatively regulates insulin secretion and is a major link between obesity, beta cell dysfunction, and type 2 diabetes. Cell. 2001; 105:745–755. [PubMed: 11440717]
18. Zhou Y, Huang H, Chang HH, Du J, Wu JF, Wang CY, et al. Induction of renal 20-hydroxyeicosatetraenoic acid by clofibrate attenuates high-fat diet-induced hypertension in rats. J Pharmacol Exp Ther. 2006; 317:11–18. [PubMed: 16339392]

NIH-PA Author Manuscript

NIH-PA Author Manuscript

NIH-PA Author Manuscript

19. Fukuda K, Tesch GH, Yap FY, Forbes JM, Flavell RA, Davis RJ, et al. MKK3 signalling plays an essential role in leukocyte-mediated pancreatic injury in the multiple low-dose streptozotocin model. Lab Invest. 2008; 88:398–407. [PubMed: 18283273]
20. Müller A, Schott-Ohly P, Dohle C, Gleichmann H. Differential regulation of Th1-type and Th2-type cytokine profiles in pancreatic islets of C57BL/6 and BALB/c mice by multiple low doses of streptozotocin. Immunobiology. 2002; 205:35–50. [PubMed: 11999343]
21. Henquin JC. Pathways in beta-cell stimulus-secretion coupling as targets for therapeutic insulin secretagogues. Diabetes. 2004; 53:S48–S58. [PubMed: 15561921]
22. Chiamvimonvat N, Ho CM, Tsai HJ, Hammock BD. The soluble epoxide hydrolase as a pharmaceutical target for hypertension. J Cardiovasc Pharmacol. 2007; 50:225–237. [PubMed: 17878749]
23. Elmarakby AA, Faulkner J, Al-Shabrawey M, Wang MH, Maddipati KR, Imig JD. Deletion of soluble epoxide hydrolase gene improves renal endothelial function and reduces renal inflammation and injury in streptozotocin-induced type 1 diabetes. Am J Physiol. 2011; 301:R1307–R1317.
24. Morisseau C. Role of epoxide hydrolases in lipid metabolism. Biochimie. 2013; 95:91–95. [PubMed: 22722082]
25. Wagner K, Inceoglu B, Hammock BD. Soluble epoxide hydrolase inhibition, epoxygenated fatty acids and nociception. Prostaglandins Other Lipid Mediat. 2011; 96:76–83. [PubMed: 21854866]
26. Simpkins AN, Rudic RD, Schreihofer DA, Roy S, Manhiani M, Tsai HJ, et al. Soluble epoxide inhibition is protective against cerebral ischemia via vascular and neural protection. Am J Pathol. 2009; 174:2086–2095. [PubMed: 19435785]
27. Roman RJ. P450 metabolites of arachidonic acid in the control of cardiovascular function. Physiol Rev. 2002; 82:131–185. [PubMed: 11773611]
28. Huang H, Morisseau C, Wang J, Yang T, Falck JR, Hammock BD, et al. Increasing or stabilizing renal epoxyeicosatrienoic acid production attenuates abnormal renal function and hypertension in obese rats. Am J Physiol. 2007; 293:F342–F349.
29. Ohtoshi K, Kaneto H, Node K, Nakamura Y, Shiraiwa T, Matsuhisa M, et al. Association of soluble epoxide hydrolase gene polymorphism with insulin resistance in type 2 diabetic patients. Biochem Biophys Res Commun. 2005; 331:347–350. [PubMed: 15845398]
30. Chen D, Whitcomb R, MacIntyre E, Tran V, Do ZN, Sabry J, et al. Pharmacokinetics and pharmacodynamics of AR9281, an inhibitor of soluble epoxide hydrolase, in single- and multiple-dose studies in healthy human subjects. J Clin Pharmacol. 2012; 52:319–328. [PubMed: 21422238]
31. Liu JY, Park SH, Morisseau C, Hwang SH, Hammock BD, Weiss RH. Sorafenib has soluble epoxide hydrolase inhibitory activity, which contributes to its effect profile in vivo. Mol Cancer Ther. 2009; 8:2193–2203. [PubMed: 19671760]

NIH-PA Author Manuscript
NIH-PA Author Manuscript
NIH-PA Author Manuscript

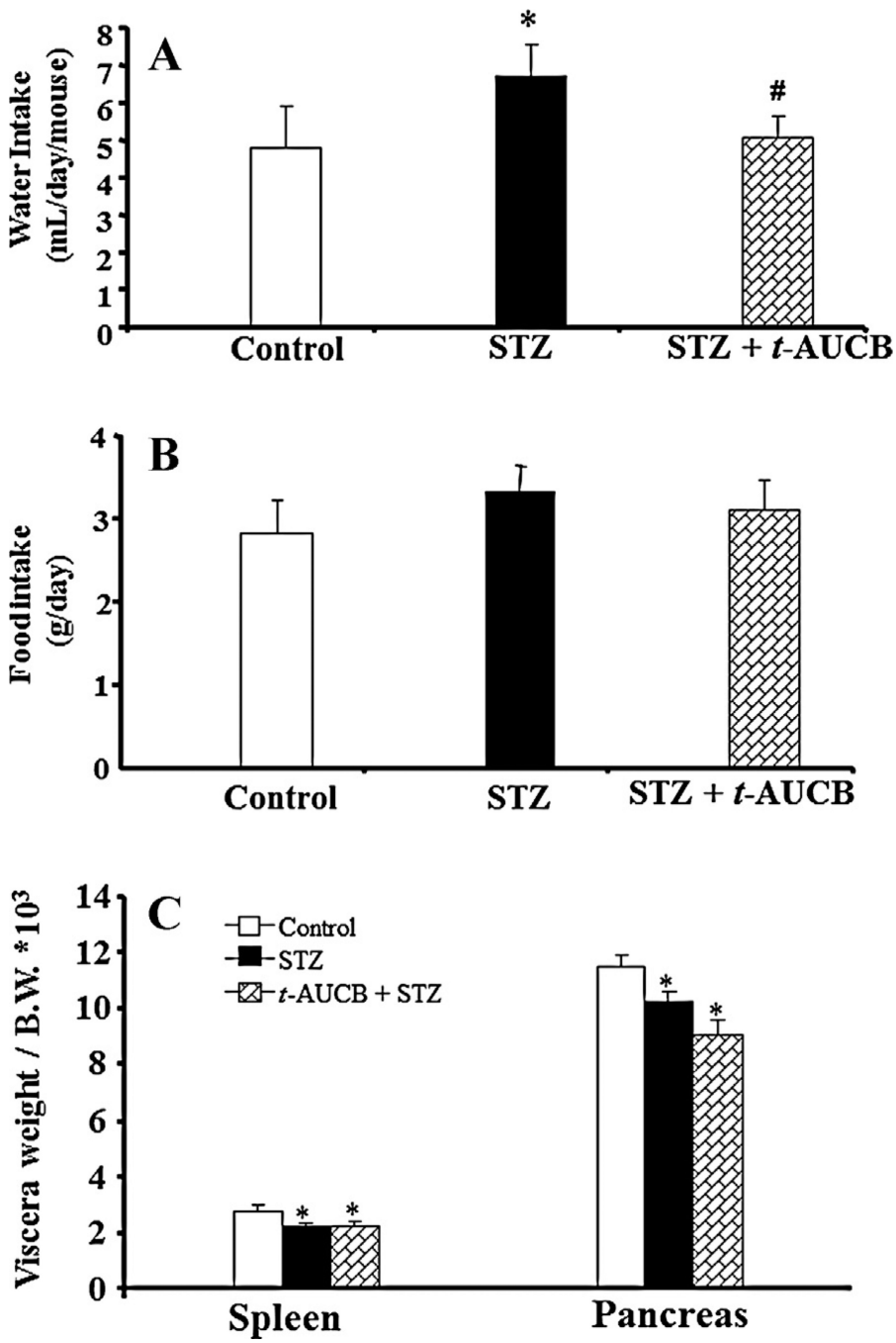

Figure 1.

Water intake (A), food intake (B), and the weight ratio of spleen and pancreas (C) in mice with STZ-induced diabetes receiving daily ip injections over 4 weeks with either vehicle or 5 mg/kg/day of *t*-AUCB. The values of water and food intake were based on the average of daily water and food intake after STZ treatment. The weight ratio of spleen or pancreas to body weight (B.W.) was determined after 4 weeks of STZ treatment. The body weight in control, STZ, and *t*-AUCB + STZ are 21 ± 0.5 g, 21.3 ± 0.5 g, and 20.8 ± 0.7 g,

NIH-PA Author Manuscript

NIH-PA Author Manuscript

NIH-PA Author Manuscript

respectively. The values are expressed as mean ± SE (n = 6). *P < 0.05, ***P < 0.001 versus control; $^{\#}P$ < 0.05, $^{\#\#\#}P$ < 0.001 versus STZ treatment.

NIH-PA Author Manuscript

NIH-PA Author Manuscript

NIH-PA Author Manuscript

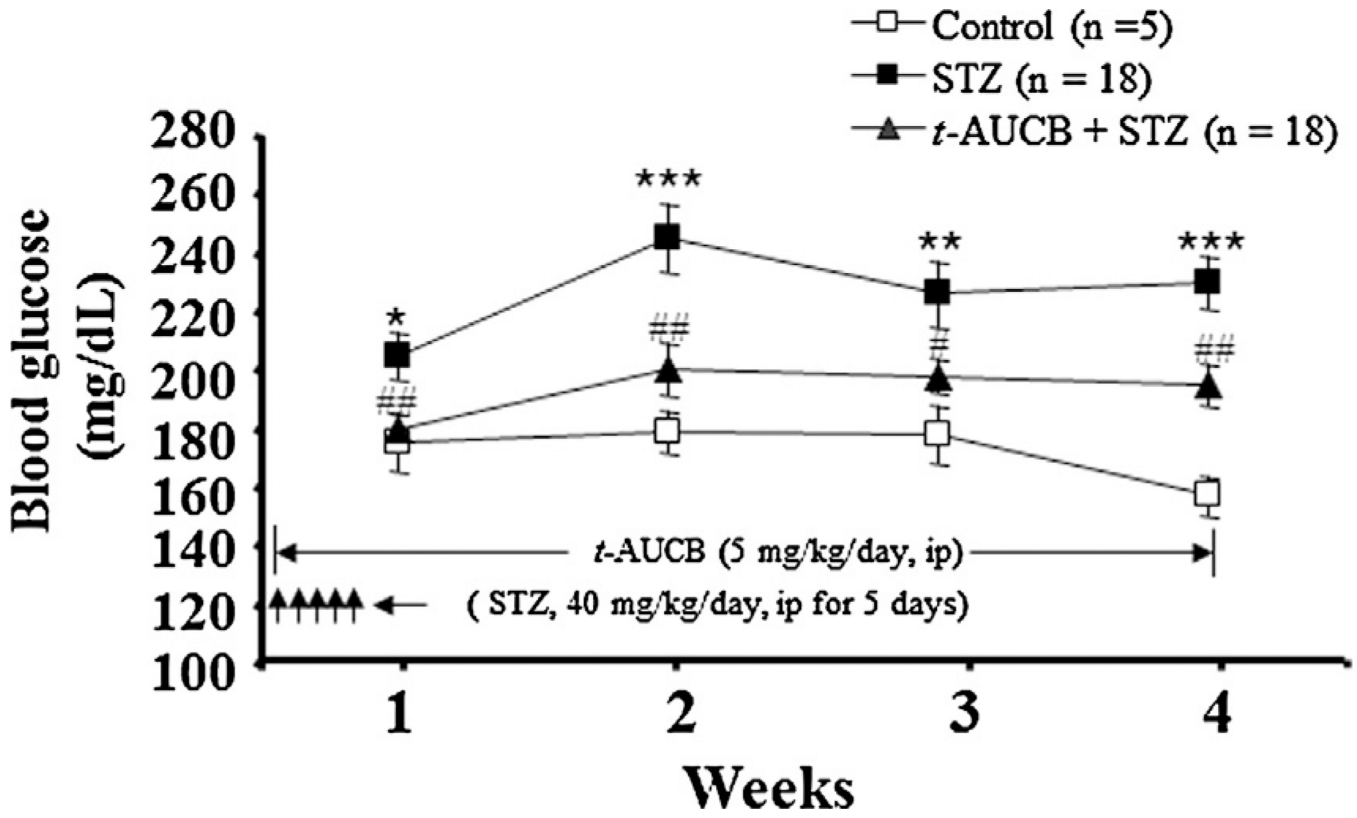

Figure 2.

Weekly blood glucose levels of mice treated with vehicle, STZ, or STZ + *t*-AUCB. The results are expressed as the mean ± SE. **P* < 0.05, ***P* < 0.01, ****P* < 0.001 versus control; $^{\#}P < 0.05$, $^{\#\#}P < 0.01$ versus STZ-treated mice.

NIH-PA Author Manuscript
NIH-PA Author Manuscript
NIH-PA Author Manuscript

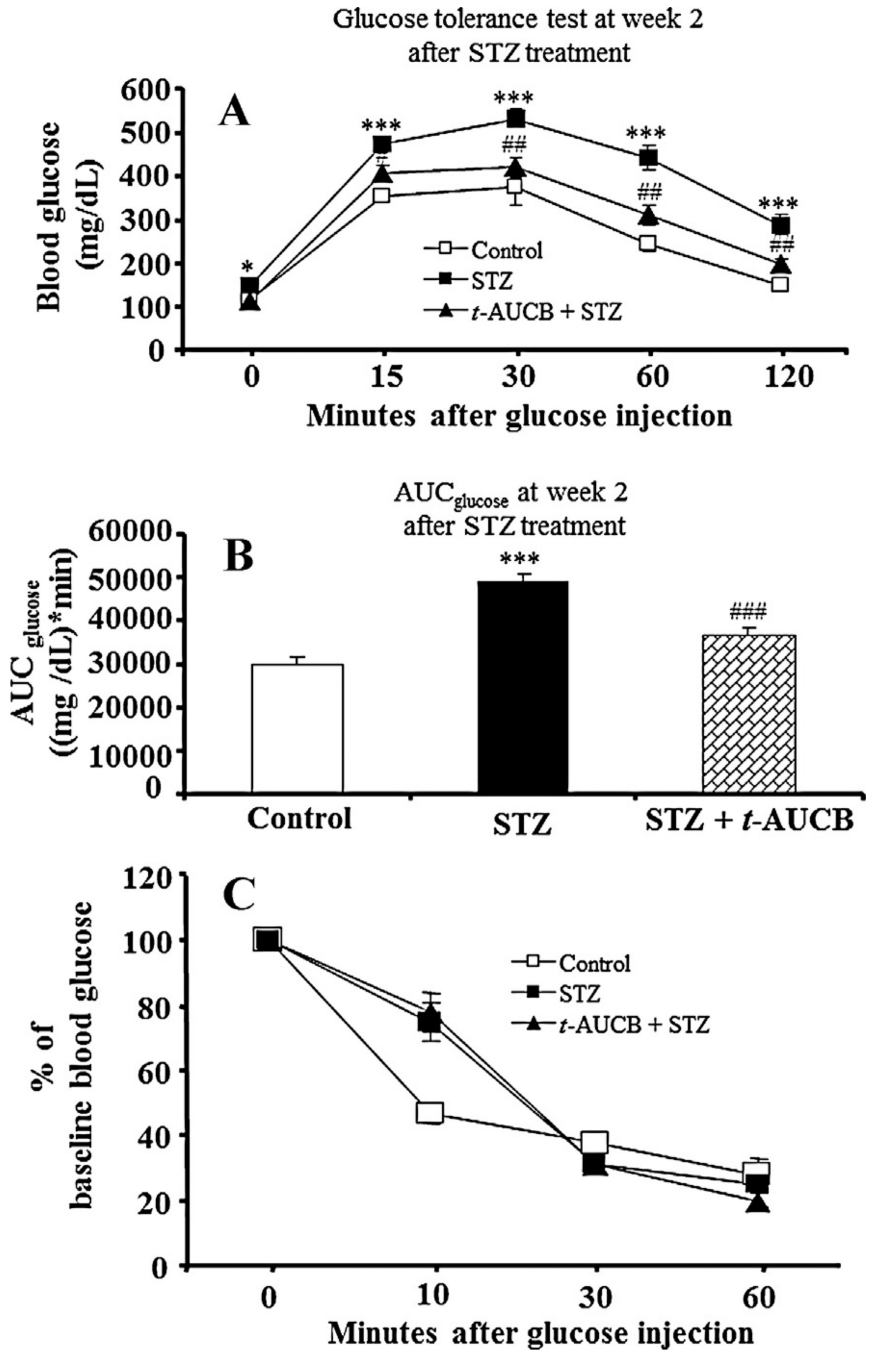

Figure 3.

(A) Intraperitoneal glucose tolerance tests at week 2 after STZ treatment. After a 6-h fast, mice (n = 6) from each group were given an ip injection of 1 g/kg of glucose. Blood glucose was measured before and at varying times after glucose administration. (B) The value of the area under the curve for blood glucose ($AUC_{glucose}$) for glucose tolerance test in different groups. (C) Intraperitoneal insulin tolerance tests at week 2 after STZ treatment. After a 6-h fast, mice (n = 6) from each group were given an ip injection of 1 U/kg of human insulin. The values of decrease ratios for each group were calculated by dividing the blood glucose

level after insulin injection by the initial blood glucose. Results are expressed as the mean ± SE. *$P < 0.05$, **$P < 0.01$, ***$P < 0.001$ versus control; $^{\#}P < 0.05$, $^{\#\#}P < 0.01$ versus STZ-treated mice.

NIH-PA Author Manuscript
NIH-PA Author Manuscript
NIH-PA Author Manuscript

NIH-PA Author Manuscript

NIH-PA Author Manuscript

NIH-PA Author Manuscript

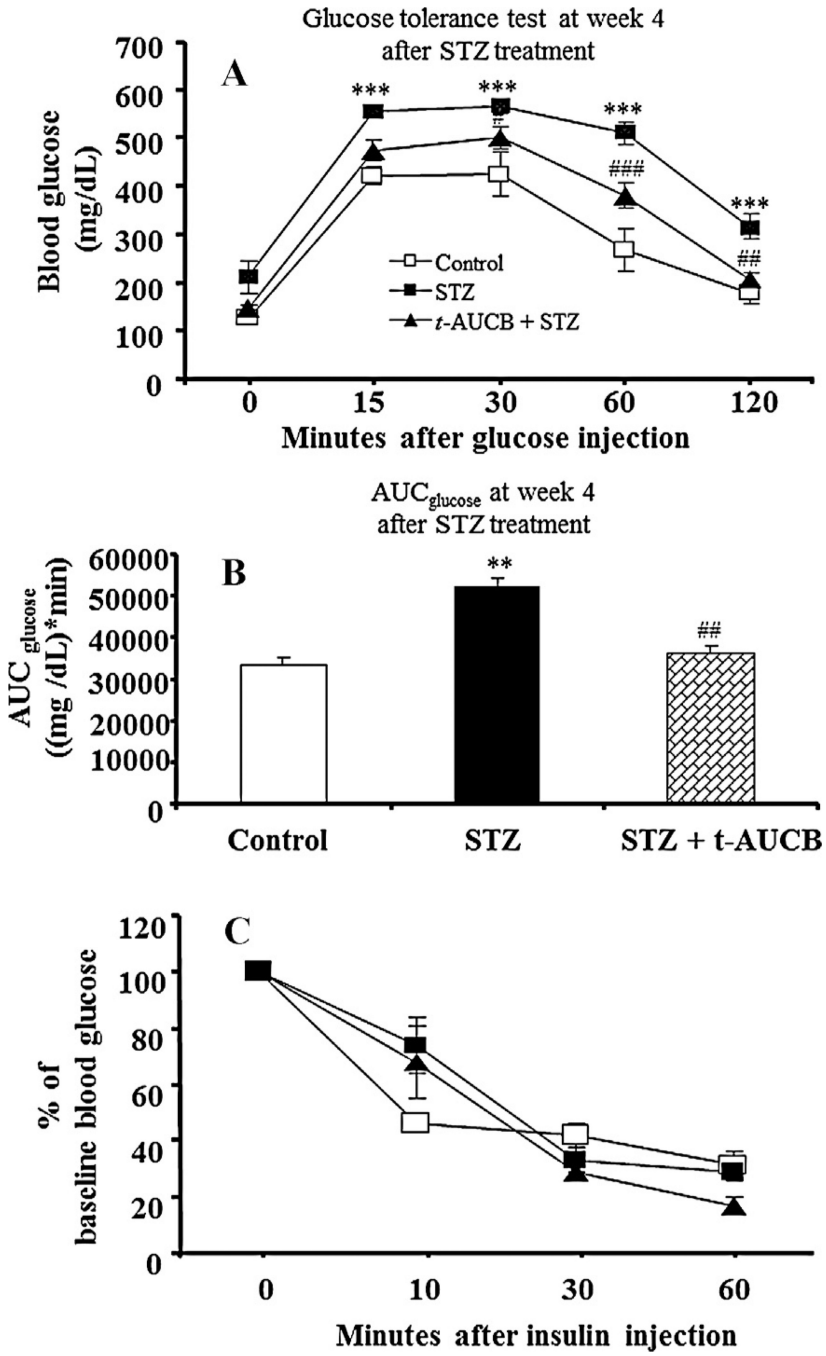

Figure 4.

(A) Intraperitoneal glucose tolerance tests at week 4 after STZ treatment. After a 6-h fast, mice (n = 6) from each group were given an ip injection of 1 g/kg of glucose. Blood glucose was measured before and at varying times after glucose administration. (B) The value of the area under the curve for blood glucose ($AUC_{glucose}$) for glucose tolerance test in different groups. (C) Intraperitoneal insulin tolerance tests at week 4 after STZ treatment. After a 6-h fast, mice (n = 6) from each group were given an ip injection of 1 U/kg of human insulin. The values of decrease ratios for each group were calculated by dividing the blood glucose

level after insulin injection by the initial blood glucose. The results are expressed as the mean ± SE. $^{*}P < 0.05$, $^{**}P < 0.01$, $^{***}P < 0.001$ versus control; $^{\#}P < 0.05$, $^{\#\#}P < 0.01$, $^{\#\#\#}P < 0.001$ versus STZ-treated mice.

NIH-PA Author Manuscript
NIH-PA Author Manuscript
NIH-PA Author Manuscript

NIH-PA Author Manuscript

NIH-PA Author Manuscript

NIH-PA Author Manuscript

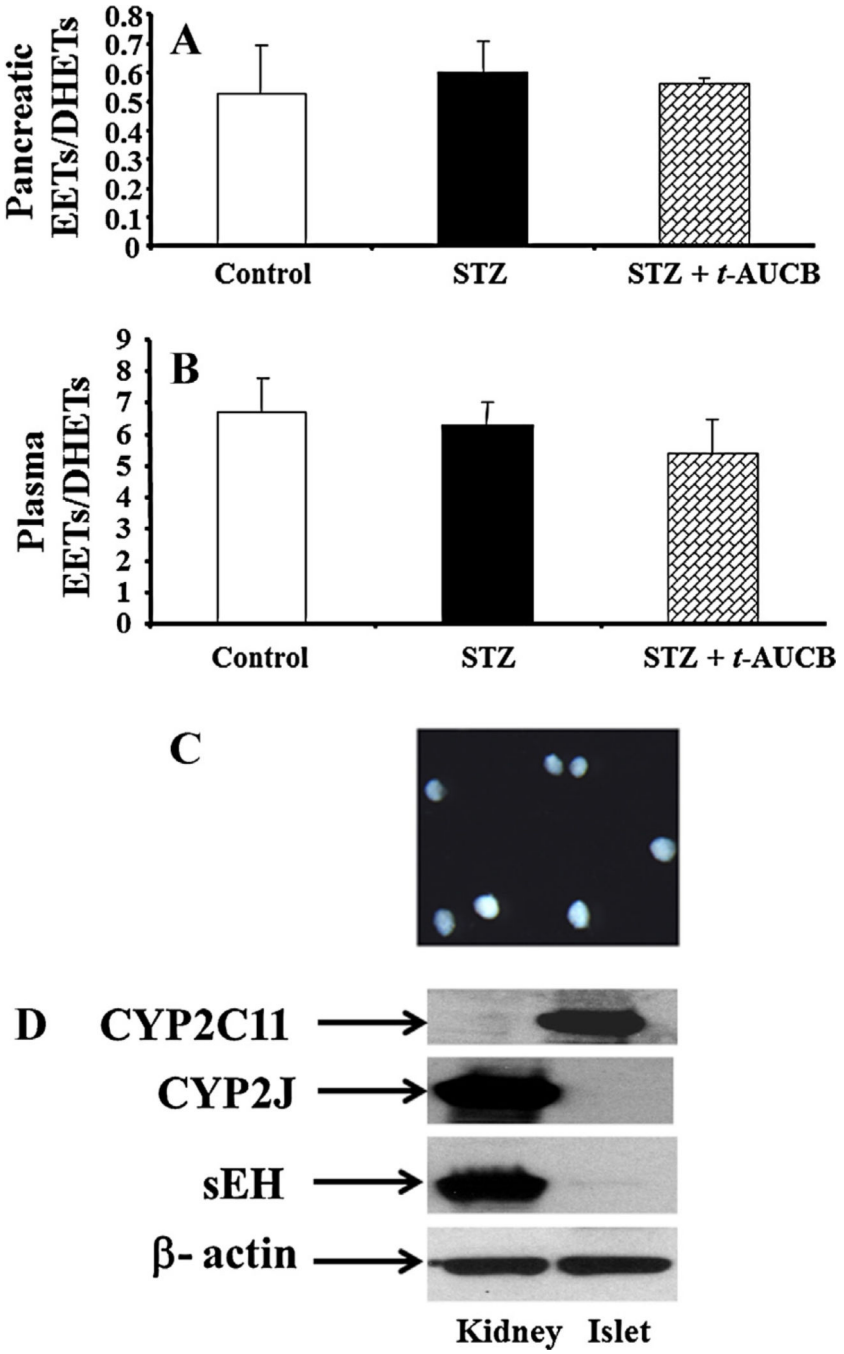

Figure 5.

(A) Pancreatic and (B) plasma ratios of EETs to DHETs ratios in mice given different treatments. After 4 weeks of different treatments, pancreatic samples were collected. LC/MS was used to measure the ratio of pancreatic EETs to DHETs. The levels of EETs and DHETs production in pancreatic samples of the control group were 0.77 ± 0.17 and 1.47 ± 0.27 ng/mg protein/h, respectively. The levels of EETs and DHETs production in plasma samples of the control group were 47 ± 8 and 7 ± 0.9 nM, respectively. (C) The

representative image of isolated islets under a dissection microscope. (D) Western blots of CYP2C11, CYP2J, and sEH in mouse kidney (30 μg) and islets (30 μg).

NIH-PA Author Manuscript
NIH-PA Author Manuscript
NIH-PA Author Manuscript

NIH-PA Author Manuscript
NIH-PA Author Manuscript
NIH-PA Author Manuscript

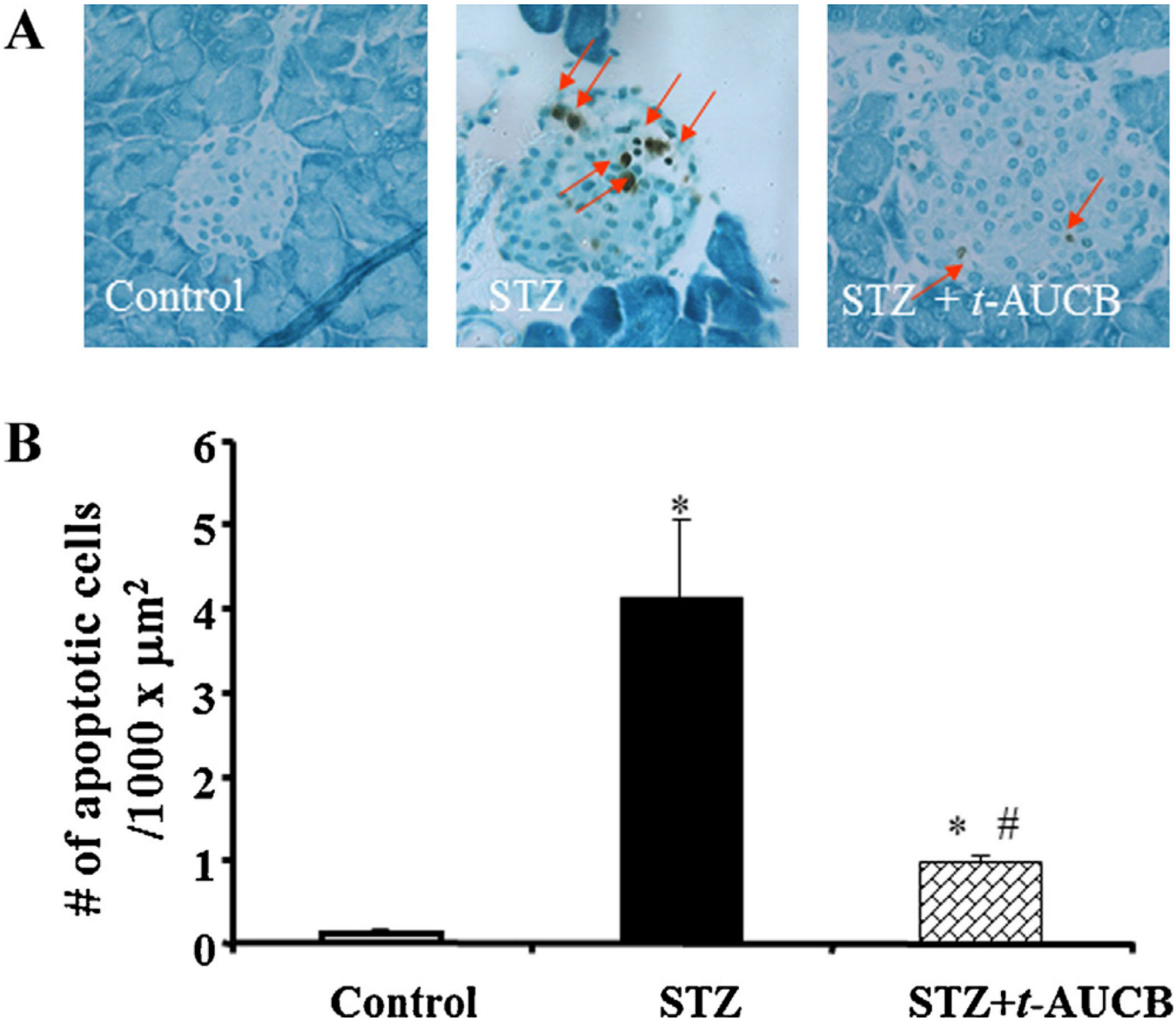

Figure 6.

(A) In control mice, pancreases showed no apoptotic cells. On day 5 after STZ treatment, a significant increase of apoptotic cells was observed in the islets of STZ mice. Also, *t*-AUCB treatment reduced apoptotic cells in islets isolated from STZ + *t*-AUCB group. (B) Quantification of TUNEL assay showed that islet cell apoptosis in the STZ + *t*-AUCB group was significantly lower than that in the STZ group. $n = 6$, $^{*}P < 0.05$ versus control group; $^{\#}P < 0.05$ versus STZ group.